

CARBONATED AND CHLORIDE CONTAMINATED CONCRETE STRUCTURE: THE ROLE OF MOLYBDENUM IN CORROSION OF STAINLESS STEEL REINFORCEMENT[#]

Artigo submetido em Março de 2013 e aceite em Abril de 2013

A. Araujo^{(1)(*)}, T. J. Mesquita⁽²⁾, E. Chauveau⁽²⁾, M. Mantel⁽²⁾, Z. Panossian⁽¹⁾, C. A. Santos⁽¹⁾ and R. P. Nogueira⁽³⁾**Abstract**

This paper is a contribution to the understanding of the role of molybdenum (Mo) in the pitting corrosion resistance of stainless steels in concrete contaminated with chloride ions after its carbonation. For the study, samples of ferritic, austenitic and duplex stainless steels were produced in laboratory with controlled levels of molybdenum (Mo). Samples of these steels were immersed in simulated carbonated and noncarbonated concrete pore solutions, both with the addition of 3.5 % of NaCl. Other samples were embedded in concrete that was later carbonated and immersed in NaCl solution. The performance of the steels in concrete was verified through corrosion potential monitoring (several months) followed by electrochemical experiments (anodic polarization). Finally, the optical and electronic microscopy techniques were used to analyze the corrosion attacked surfaces.

Keywords: Corrosion, Concrete Structures, Stainless Steel, Molybdenum, Carbonation, Chloride Ions, Localized Corrosion

ESTRUTURAS DE CONCRETO CARBONATADO E CONTAMINADO COM CLORETO: A INFLUÊNCIA DO MOLIBDÊNIO NA CORROSÃO DE ARMADURA DE AÇO INOXIDÁVEL

Resumo

Este trabalho é uma contribuição ao estudo da influência do molibdênio (Mo) na resistência à corrosão por pite de aços inoxidáveis em concreto contaminado por íons cloreto, após a sua carbonatação. Para o estudo, amostras de aços inoxidáveis ferrítico, austenítico e dúplex foram preparadas em laboratório com níveis controlados de Mo. Amostras desses aços foram imersas em soluções alcalinas simulando água de poros de concreto carbonatado e não carbonatado, ambas com adição de 3,5 % de NaCl. Outras amostras foram embutidas em concreto, posteriormente carbonatado e imerso

em solução de NaCl. O desempenho dos aços foi verificado pela monitorização do potencial de corrosão (vários meses), seguido de ensaios eletroquímicos como de polarização anódica. Finalmente, os microscópios óptico e eletrônico foram usados para analisar as superfícies das armaduras atacadas pela corrosão.

Palavras Chave: Corrosão, Estruturas de Concreto, Aço Inoxidável, Molibdenio, Carbonatação, Íons Cloreto, Corrosão Localizada

1. INTRODUCTION

A large part of the world-wide transport and energy infrastructures uses reinforced concrete. Its durability is due to the excellent chemical stability of hydrated Portland cement and the passivity of carbon steel in the alkaline pore solution of concrete with a pH from 10 to 13.5. Corrosion of the reinforcement steels, induced by chloride ions penetrating into the concrete, is the main cause of early damage, loss of serviceability and safety of reinforced concrete structures [1, 2]. In order to prevent reinforcement steel corrosion in highly aggressive environments, the use of stainless steels (SS) reinforcing bars is becoming increasingly popular as they present much higher pitting corrosion resistance in concrete than carbon steel reinforcing bars. Furthermore, higher chloride content is required to initiate the localized corrosion and to depassivate the stainless steels surface [3]. The localized corrosion (pitting and crevice) and generalized attack of the steels are associated with chloride ions and pH lowering due to carbonation processes, respectively [4]. Thus, when the reinforced concrete structure is exposed to chloride contaminated environments and a fast carbonation process; the stainless steel reinforcing bars are probably a good choice to avoid several corrosion problems.

In this context, the improvement of the SS corrosion resistance is the major priority, therefore the molybdenum (Mo) as an alloy element is a suitable metal to play this role. It has long been known that Mo additions in SS improve their corrosion resistance and also in favor of an easier repassivation [5-8]. Although there are several studies about

electrochemical behavior of Mo and its role to increase the corrosion properties of the SS in acidic media, earlier studies showed an absence of the beneficial effect of Mo on pitting corrosion resistance of austenitic SS in alkaline solutions [1].

The studies of Ilevbare *et al.* [9] explain the action of Mo principally on nucleation and metastable pitting corrosion of austenitic SS. As these steps of pitting corrosion constitute the early stage of a pit growing, the probability associated with the successful generation of these events will affect the onset of stable pitting. According to Pardo *et al.* [6], the Mo addition enhances the pitting corrosion resistance of austenitic SS in 3.5 w % NaCl, because this element progressively reduces the corrosion rate, increasing the CPT (Critical Pitting Temperature) values and ennobling both the break potential (E_{pit}) and the corrosion potential (E_{corr}). Moreover, these authors believe that Mo promotes an important role on the repassivation process and, consequently, decreases the pitting propagation by formation of Mo oxides on the pit walls. These results are in agreement with the studies done by Lemaitre *et al.* [10] which describe the beneficial effect of the Mo addition on both in ferritic and austenitic SS regarding the resistance to local breakdown of the passive film in neutral solutions. On the other hand, in alkaline medium, the Mo addition seems to have no positive effect on austenitic SS [1, 11, 12]. However, the electrochemical experiments done in solutions simulating the concrete environments are not really representative of the real conditions. Therefore, a method to study the corrosion properties of stainless steels in contaminated concrete environments is being developed by the European Community.

Under this context, the aim of the present paper is to characterize the performance of the different stainless steel classes (austenitic, ferritic and mainly duplex) in a carbonated and chloride-contaminated concrete. Several-month surveys of corrosion potential followed by electrochemical experiments as well as microscopy analyses were done. Finally, the roles of the Mo addition on these different SS types were investigated in those aggressive corrosion conditions.

[#]Paper presented at the EUROCORR 2012.

2. EXPERIMENTAL METHODOLOGY

2.1. Materials

Three different classes of stainless steels (austenitic, ferritic and duplex) were studied. A free Mo (0 wt% Mo) and Mo containing (3 wt% Mo) alloys were produced by UGITECH research center for each SS type in order to eliminate all concentration variations of other elements, for example Cr, Ni, N and Mn. These elements may have a big influence on the corrosion resistance of these alloys and then may disturb the analysis of the real role of Mo effect on SS corrosion and passivation properties. Thus, it was decided to fabricate these materials under highly controlled laboratory conditions based on the traditional industrial SS compositions, such as EN 1.4016 and EN 1.4113 for ferritic SS, EN 1.4307 and EN 1.4404 for austenitic SS, and finally, EN 1.4362 and EN 1.4462 for duplex ones (austeno-ferritic).

In order to simplify the writing and reading of this work, the lab alloy samples were named by using their chemical composition values for the main SS alloying elements, Cr, Ni and Mo. For example, if the material contains 18 wt % of Cr, 12 wt % of Ni and 3 wt % of Mo, it is named 18Cr12Ni3Mo which represents an austenitic SS (Cr+Ni) with 3 % of Mo. Table 1 presents the chemical composition of the studied alloys.

Table 1 - Chemical composition of laboratory stainless steels produced by UGITECH research center.

Laboratory Material		Elements (wt.%)									
		C	Si	Mn	Ni	Cr	Mo	N	Al	S (ppm)	PREn
Austenitic	18Cr12Ni	0.025	0.594	1.012	12.067	17.999	0.004	0.023	0.0033	13	18.38
	18Cr12Ni1Mo	0.028	0.513	0.990	12.060	17.859	1.000	0.024	0.0031	13	21.54
	18Cr12Ni2Mo	0.020	0.515	1.048	12.080	17.879	1.968	0.019	0.0032	12	24.68
	18Cr12Ni3Mo	0.028	0.571	1.018	11.995	18.003	2.989	0.029	0.0036	15	28.33
Ferritic	18Cr	0.028	0.492	1.056	0.003	18.108	0.004	0.029	0.0024	15	18.59
	18Cr3Mo	0.029	0.533	1.076	0.005	18.018	3.01	0.028	0.0023	14	28.399
Duplex	23Cr4.6Ni	0.029	0.58	1.031	4.569	22.968	0.015	0.175	0.0024	12	25.82
	23Cr4.6Ni3Mo	0.029	0.559	0.981	4.56	22.97	3.004	0.186	0.003	13	35.86

All materials were hot forged, hot rolled, annealed and then cold rolled. Finally, specimens were sampled from the laboratory cold laminated boards in disk form (diameter 1.5 cm and thickness 2 mm). Prior to general corrosion tests, specimens were polished up to 1200 grid emery papers, degreased with alcohol, rinsed with distilled water and dried with hot air. In order to have a first approach of pitting corrosion resistance of these materials, the PREn values were calculated by the following equation:

PREn = %Cr + 3.3 %Mo + 16 %N

The obtained values are also presented in Table 1. This widely used PREn expression is linked to the content of the three most important elements, Cr, Mo and N, to the pitting corrosion resistance. So, for all three SS families, the addition of 3 % Mo increases the PREn values by about 10 points.

2.2. Sample preparation

The stainless steel disks (1.5 cm and 2 mm as diameter and thickness, respectively) were embedded in an acrylic resin after connecting to it a small copper wire in order to have a good electrical contact to perform the electrochemical experiments. Fig. 1 illustrates a typical SS sample preparation before covering them with concrete. This procedure provided a working electrode area of 1.77 cm² as only one side of the SS disk were exposed to the concrete. It is worth mentioning that the rolling deformation direction of the studied SS was evaluated.

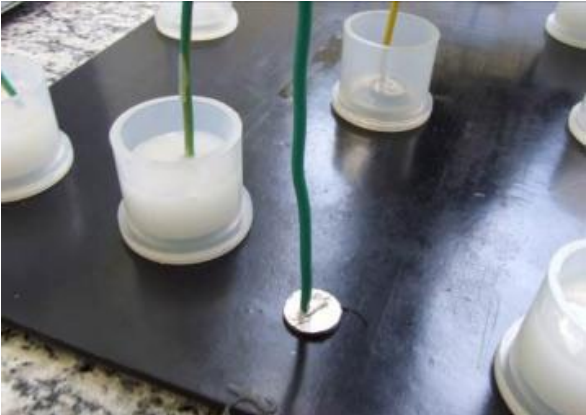


Fig.1 - Laboratory stainless steel specimens during the preparation for electrochemical experiments.

The resin-embedded SS specimens were covered by concrete. For each SS, ten concrete-covered samples were prepared. This number of samples was defined because in a previous study [13], it was verified that a high variation in electrochemical responses occurs when concrete-covered metallic specimens are tested. The shape of the concrete samples was cylindrical with 7 cm in diameter and 3 cm in height. The concrete sample preparation is illustrated in Fig. 2.



Fig. 2 - Laboratory resin embedded stainless steel specimens being covered by concrete.

Micro-concrete was used for the concrete-covered sample preparation. This concrete presents a compressive strength of 12 MPa (tested under ABNT NBR 5739 conditions [14]). The main components of this micro-concrete are presented in Table 2.

Table 2 - Micro-concrete components.

Components	Standard
First Sand	NBR NM 248 [15]
Medium Sand	NBR NM 248 [15]
Cement CP II E32	ABNT NBR 11578 [16]

After curing of concrete samples, they were exposed to CO_2 and then to chloride ions. The CO_2 exposure was performed in a controlled carbonation chamber (at 25 °C, at 65 % of relative humidity and at 2 % CO_2) as shown in Fig. 3a, and the contamination of concrete with chloride ions was performed by partial immersion of concrete covered samples in a brine solution (35 g L^{-1} of NaCl), as shown in Fig. 3b. During the wet curing of concrete samples and also while the immersion in saline solution, the E_{corr} was monitored (Fig. 3c).

The carbonation of concrete samples was done in two cycles. First, the samples were exposed to the carbonation chamber for 8 days (first cycle) followed by exposure of the chloride ions for 114 days. As mentioned, during the exposure to the chloride ions the E_{corr} was monitored.

After 114 days in chloride solution, one sample of each type of the studied alloys was fractured. A visual inspection and a phenolphthalein-carbonation test were performed with the fractured samples. No corrosion of the studied alloys was observed. Additionally, it was verified that the carbonation front did not reach the surface of the embedded metallic alloys, i.e., the carbonation was not completed in the first cycle of carbonation. For this reason, a second carbonation cycle (second cycle) was performed. In this case, the samples were exposed to the carbonation chamber for 36 days followed by exposure to chloride ions during which the E_{corr} was again monitored.

The interpretation of the E_{corr} values is not an easy task, but its progression with time may provide an important information about the passivation behavior of the stainless steel surface. Normally, a decrease of the E_{corr} with time is associated with a depassivation of the surface (corrosion) whereas its increase with time is attributed to surface passivation (formation of Cr oxides).

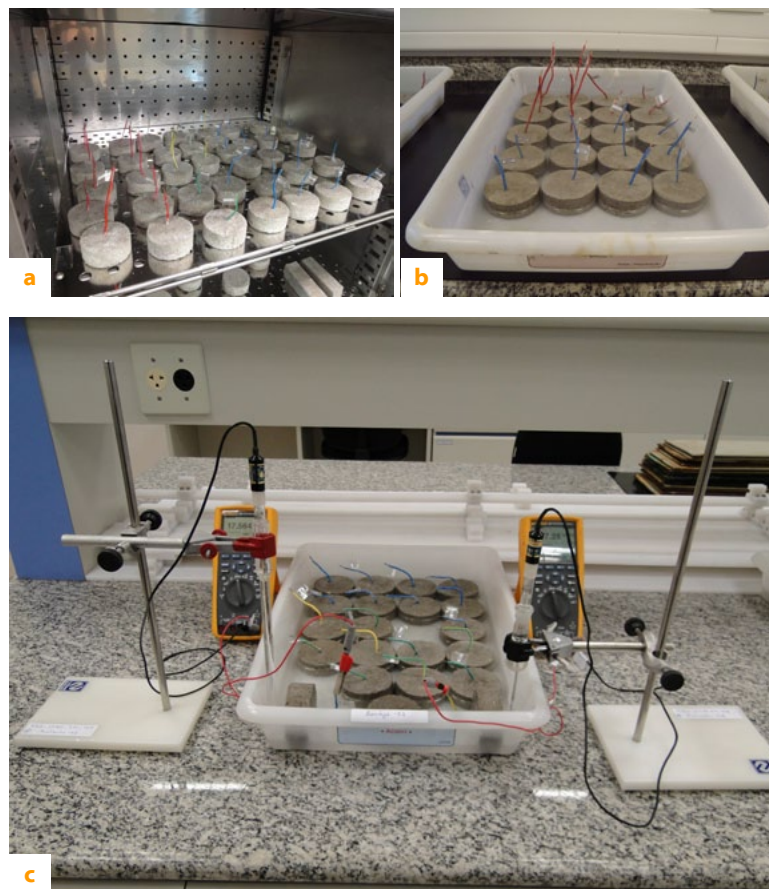


Fig. 3 - (a) Reinforced concrete samples exposed to carbon dioxide in a carbonation chamber. (b) Partial immersion of the reinforced concrete samples in saline solution. (c) Corrosion potential monitoring during the immersion period.

2.3. Electrochemical measurements

Electrochemical measurements (anodic polarization curves) were performed using the reinforced concrete samples. A potentiostat/galvanostat SOLARTRON, Schlumberger model SI 1287 Electrochemical Interface Potentiostat and an adapted three-electrode cell were used to carry out these experiments. The reference electrode was a saturated calomel electrode (SCE) and a Pt grid was used as the counter electrode. The test cell was kept in a Faraday cage in order to avoid environmental noises (Fig. 4). Potentiodynamic anodic polarization experiments were performed at a scan rate of 1 mV s^{-1} , starting at -30 mV with respect to the corrosion potential (E_{corr}).

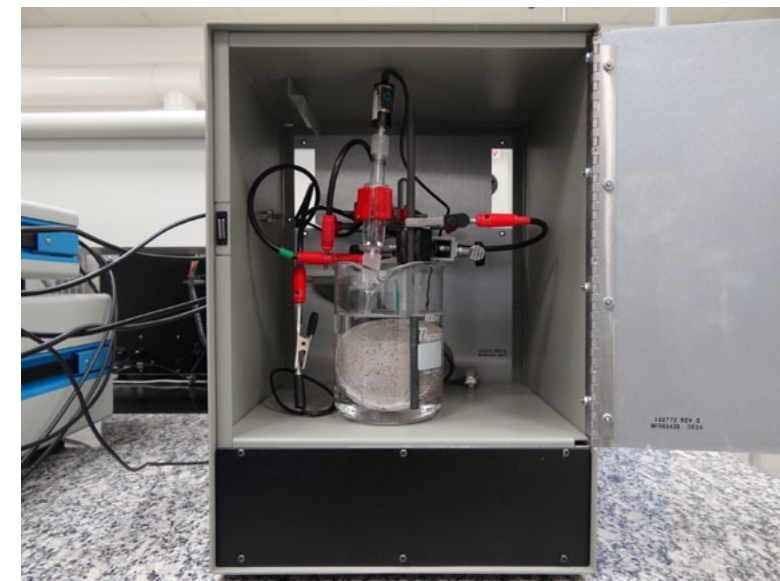


Fig. 4 - Test cell in a Faraday cage.

2.4. Microscopic measurements

After the electrochemical tests, a visual examination of the stainless steel surface exposed to the contaminated concrete was done. This analysis was performed by using a stereoscope with a magnification capacity of 80 times and also a scanning electron microscope (SEM). In some stainless steel samples, a chemical analysis was also performed by energy dispersive spectroscopy (EDS) during the SEM investigations.

3. RESULTS AND DISCUSSION

3.1. Monitoring of corrosion potential for different stainless steels in a contaminated concrete environment

The corrosion potential (E_{corr}) of the different SS in the contaminated concrete environment was measured after the immersion in the chloride solution (after the two carbonation cycles of concrete samples). Fig. 5 and Fig. 6 show the obtained corrosion potential (E_{corr}) values for all the monitoring period (about 215 days) for the 18Cr12Ni3Mo and 18Cr12Ni austenitic stainless steels, respectively. Comparing those Figures, one can clearly observe the positive effect of Mo on the corrosion potential values.

For the 18Cr12Ni3Mo SS, the E_{corr} seems to increase a little after the first carbonation period and it is still stable after the second carbonation step, as shown in Fig. 5. This steel assumes values in the range from -300 mV_{SCE} to 100 mV_{SCE} . This range continues almost the same after the second carbonation cycle, as shown in Fig. 5. On the other hand, for the 18Cr12Ni SS, the E_{corr} decreases after the second carbonation and stays between -350 mV_{SCE} and 0 mV_{SCE} but these values decrease a lot after the second carbonation cycle, as presented in Fig. 6. The final average E_{corr} for the austenitic SS is about -85 mV_{SCE} for 18Cr12Ni3Mo and -250 mV_{SCE} for 18Cr12Ni. Thus, the presence of Mo shifted the E_{corr} of the austenitic SS toward noble values in about 200 mV when these materials are exposed to chloride-contaminated and carbonated concrete.

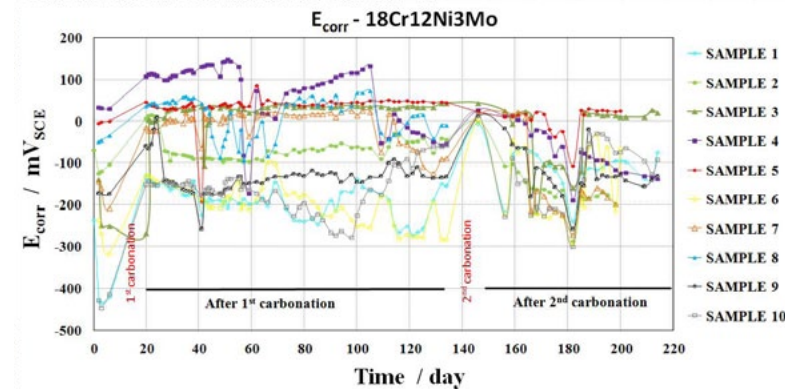


Fig. 5 - Corrosion potential measurement vs time for the ten different samples of 18Cr12Ni3Mo SS in a NaCl solution, after the first carbonation and after the second carbonation. The initial six-day period corresponds to the wet curing of the concrete samples.

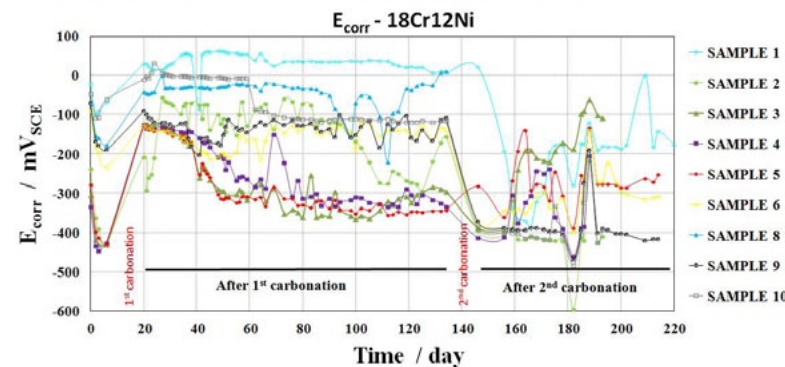


Fig. 6 - Corrosion potential measurement vs time for the ten different samples of 18Cr12Ni SS in a NaCl solution, after the first carbonation and after the second carbonation. The initial six-day period corresponds to the wet curing of the concrete samples.

Fig. 7 and Fig. 8 show the E_{corr} versus time after the two carbonation cycles for 18Cr3Mo and 18Cr ferritic SS, respectively. In these Figures, the results of the ten monitored samples for each material are presented. The Mo effect on the corrosion potential is evident when

one compares both ferritic stainless steels, even more after the second carbonation. The E_{corr} values for the 18Cr3Mo stainless steel are stable for all the monitoring period (about 215 days) however, the E_{corr} values of the 18Cr SS abruptly decrease to detrimental potentials after the second carbonation cycle. The final average E_{corr} for these SS is about -188 mV_{SCE} for 18Cr3Mo and -511 mV_{SCE} for 18Cr. Consequently, the decrease on the corrosion potential was higher than 300 mV for the ferritic SS in the absence of Mo.

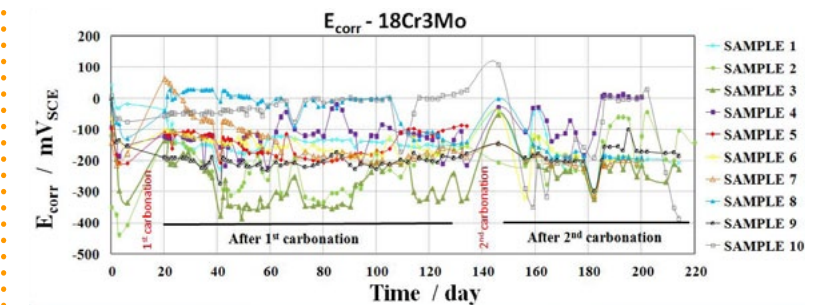


Fig. 7 - Corrosion potential measurement vs time for the ten different samples of 18Cr3Mo SS in a NaCl solution, after the first carbonation and after the second carbonation. The initial six-day period corresponds to the wet curing of the concrete samples.

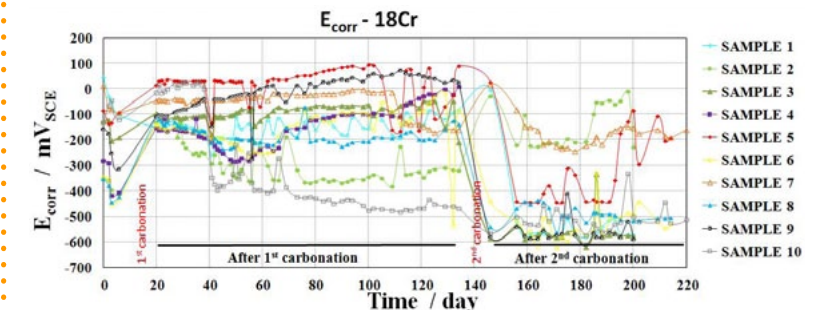


Fig. 8 - Corrosion potential measurement vs time for the ten different samples of 18Cr SS in a NaCl solution, after the first carbonation and after the second carbonation. The initial six-day period corresponds to the wet curing of the concrete samples.

Fig. 9 and Fig. 10 show the E_{corr} results for the duplex SS. Comparing these figures, one can clearly see the positive influence of Mo on the corrosion potential of duplex alloys. After the second carbonation cycle, the E_{corr} values are much higher for the 23Cr4.6Ni3Mo SS than for 23Cr4.6Ni. More specifically, the final average E_{corr} for the duplex SS is about -73 mV_{SCE} for 23Cr4.6Ni3Mo and -211 mV_{SCE} for 23Cr4.6Ni. Moreover, the shape of the E_{corr} curves seems to increase in presence of Mo – nonetheless, it seems to decrease in the absence of Mo.

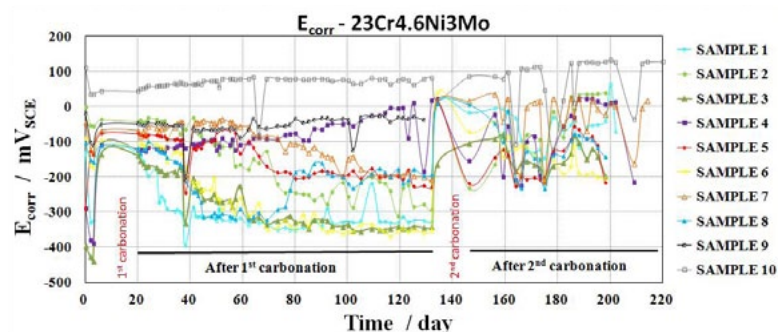


Fig. 9 - Corrosion potential measurement vs time for the ten different samples of 23Cr4.6Ni3Mo SS in the contaminated concrete environment. The initial six-day period corresponds to the wet curing of the concrete samples.

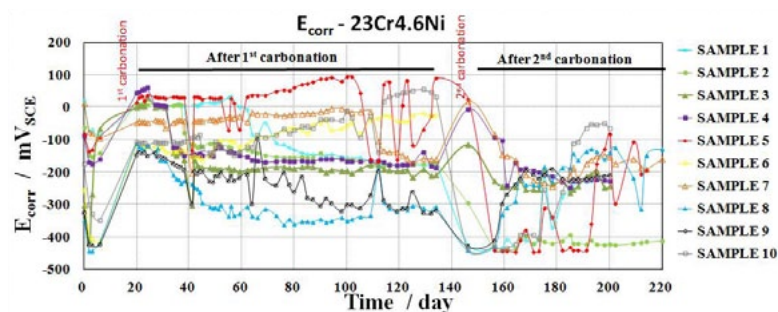


Fig. 10 - Corrosion potential measurement vs time for the ten different samples of 23Cr4.6Ni SS in the contaminated concrete environment. The initial six-day period corresponds to the wet curing of the concrete samples.

Another important point of the above discussed monitoring curves is the high dispersion of the E_{corr} values. This variation on the E_{corr} values may be associated with the high electrical resistivity of the concrete and also with the occurrence of crevice corrosion in the metal/resin interface of concrete covered samples, as is discussed in the next section. The crevice corrosion may disturb the electrochemical responses of the performed experiments.

3.2 Crevice and pitting corrosion of stainless steels in contaminated concrete environments - An electrochemical analysis

Fig. 11 shows the typical polarization curves obtained for laboratory austenitic material in the studied contaminated concrete. The polarization experiment was done for at least three samples in order to confirm the reproducibility of the obtained results. At the end of each electrochemical test, the concrete covered samples were fractured for the stainless steel surface inspection after polarization. It was verified that all the austenitic SS working electrodes presented crevice corrosion at the metal/resin interface (see examples in Table 3).

In order to verify whether the crevice corrosion occurred due to the polarization, the nonpolarized samples were also fractured. Crevice corrosion was detected in the metal/resin interface for almost all of them (see examples in Table 3). Therefore, it was concluded that when the polarization started, crevice corrosion was already established at the working electrode at the metal/resin interfaces.

Despite the crevice corrosion occurrence, it is possible to verify the huge positive effect of Mo on the corrosion resistance of austenitic grades in this carbonated and chloride-contaminated concrete, as the 18Cr12Ni SS shows a rapid current increase with the potential increase showing a clear active behavior. On the other hand, the 18Cr12Ni1Mo, 18Cr12Ni2Mo and 18Cr12Ni3Mo SS show a lower increase of the current under anodic polarization, i.e., the anodic curves of these steels are more polarized and present a lower current density level. Moreover, a clear positive effect of the Mo on the corrosion potential (E_{corr}) can be seen in Fig. 11. These results are in good agreement with the experiment conducted in the simulated concrete solution with the same samples, as described elsewhere [1, 12, 17].

Observing the nonpolarized sample surfaces shown in Table 3, the positive effect of Mo in austenitic stainless steels can clearly be observed, i.e, the intensity of the crevice corrosion decreases

with the addition of Mo. The corrosion attack on the surface of the 18Cr12Ni and on the 18Cr12Ni1Mo was easily identified in the metal/resin interface (crevice corrosion), nevertheless, the surface of the 18Cr12Ni2Mo was much less corroded and the 18Cr12Ni3Mo surface did not present crevice corrosion in all the samples.

After the electrochemical polarization experiments, all different austenitic SS presented crevice corrosion as can be seen in Table 3. However, an important detail of those images is that even after the electrochemical forced corrosion attack, the presence of Mo seems to decrease the crevice corrosion of the austenitic SS, which is a very interesting behavior.

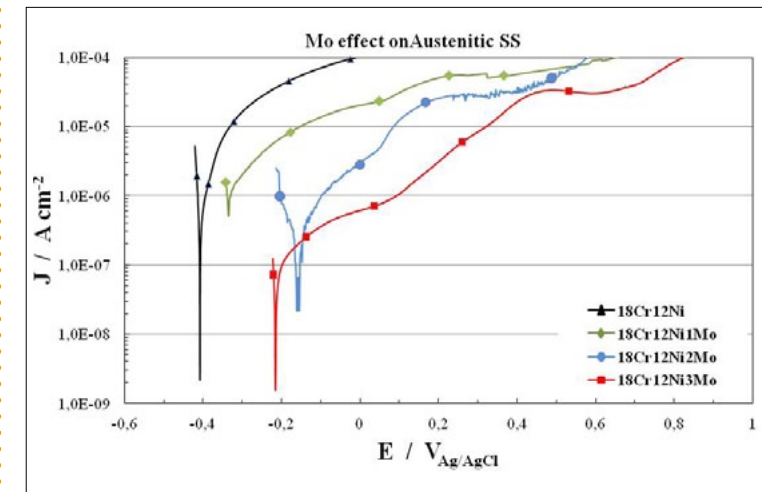


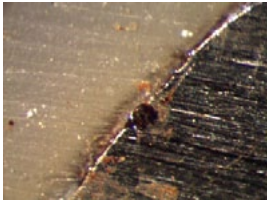

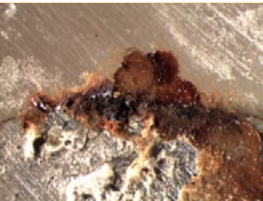
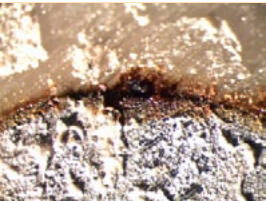




Fig. 11 - Polarization curves obtained for 18Cr12Ni (black), 18Cr12Ni1Mo (green), 18Cr12Ni2Mo (blue) and 18Cr12Ni3Mo (red) austenitic SS in the chloride-contaminated and carbonated concrete. The Mo effect can be directly observed by comparing these curves.

Fig. 12 shows the typical anodic polarization curves for 18Cr and 18Cr3Mo ferritic grade stainless steels in the studied contaminated concrete. The same behavior related to crevice corrosion was observed with the ferritic stainless steels: crevice corrosion was observed in the metal/resin interface before and after the anodic polarization.

Table 3 - Optical images of the austenitic stainless steel surfaces before and after anodic polarization.

NONPOLARIZED AUSTENITIC SS				
	18Cr12Ni – sample 2	18Cr12Ni1Mo – sample 3	18Cr12Ni2Mo – sample 7	18Cr12Ni3Mo – sample 6
E_{corr}	-417 mV _{SCE}	-330 mV _{SCE}	-186 mV _{SCE}	-64 mV _{SCE}
Images				
	Crevice corrosion	Crevice corrosion	Crevice corrosion	No sign of corrosion
AUSTENITIC SS AFTER ANODIC POLARIZATION				
	18Cr12Ni – sample 9	18Cr12Ni1Mo – sample 10	18Cr12Ni2Mo – sample 10	18Cr12Ni3Mo – sample 4
Images				
	Crevice corrosion	Crevice corrosion	Crevice corrosion	Crevice corrosion

From Fig. 12, a positive effect of Mo on the corrosion resistance of the ferritic SS can again be observed despite the crevice corrosion occurrence. The most evident positive effect is the significant increase of the E_{corr} (more than 400 mV). Additionally, a slight decrease of the corrosion current (i_{corr}) due to the addition of Mo is observed. These results are in agreement with the preliminary results obtained with the same material in a synthetic concrete pore solution as described elsewhere [1, 12, 17].

- The images presented in Table 4 illustrate the surface of the ferritic SS samples before (nonpolarized) and after the polarization measurements. As for the austenitic SS, the positive effect of Mo can be clearly observed in both before and after the polarization measurements. The surface of the 18Cr SS presented severe crevice corrosion in the metal/resin interface before (nonpolarized) and after the polarization nevertheless, the 18Cr3Mo SS presented slight crevice corrosion in the metal/resin interface in both cases.

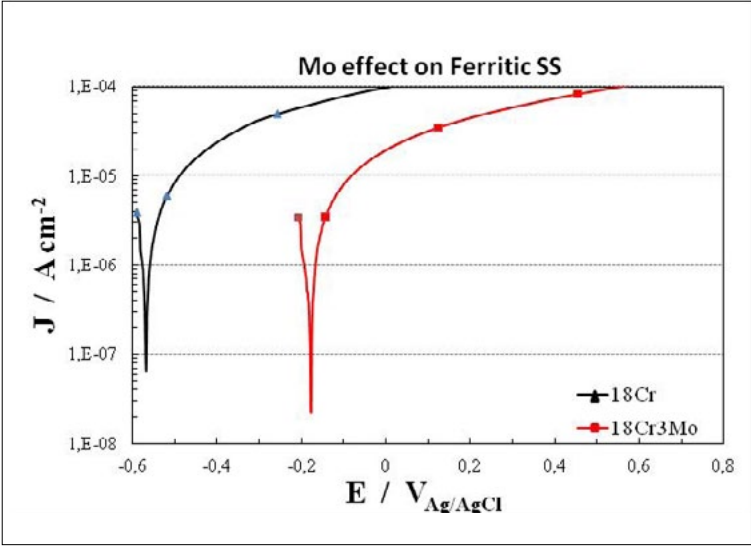






Fig. 12 - Polarization curves obtained for 18Cr (black curve) and 18Cr3Mo (red curve) ferritic SS in the chloride-contaminated and carbonated concrete. The Mo effect can be directly observed by comparing these curves.

The beneficial effect of the Mo addition on the corrosion resistance of duplex SS was also detected as can be observed in Fig. 13 and Table 5. From Fig. 13, it can be seen that the 23Cr4.6Ni presents an active behavior and 23Cr4.6Ni3Mo presents a passive behavior. It is worth noticing that the Mo effect was very high for the duplex stainless steel as no current increase was observed in the passive region up to potential equal to 0.9 V_{SCE} (potential at which the oxygen evolution occurs). This means that the 23Cr4.6Ni3Mo was not attacked during the anodic polarization (the increase on the current is due to the oxygen evolution) nonetheless the 23Cr4.6Ni presented corrosion from the beginning of the polarization.

This statement may be ascertained by the optical verification of the duplex sample surfaces before (nonpolarized) and after the anodic polarization as shown in Table 5. The 23Cr4.6Ni SS presented crevice corrosion in both cases in all samples, however, the 23Cr4.6Ni3Mo SS presented no corrosion attack on the surface of some samples nonpolarized.

Table 4 - Optical images of the ferritic stainless steel surfaces before and after anodic polarization.

NONPOLARIZED FERRITIC SS		
	18Cr – sample 9	18Cr3Mo – sample 3
E_{corr}	-590 mV _{SCE}	-250 mV _{SCE}
Images		
	Severe Crevice Corrosion	Slight Crevice Corrosion
FERRITIC SS AFTER ANODIC POLARIZATION		
	18Cr – sample 7	18Cr3Mo – sample 9
Images		
	Severe Crevice Corrosion	Slight Crevice corrosion

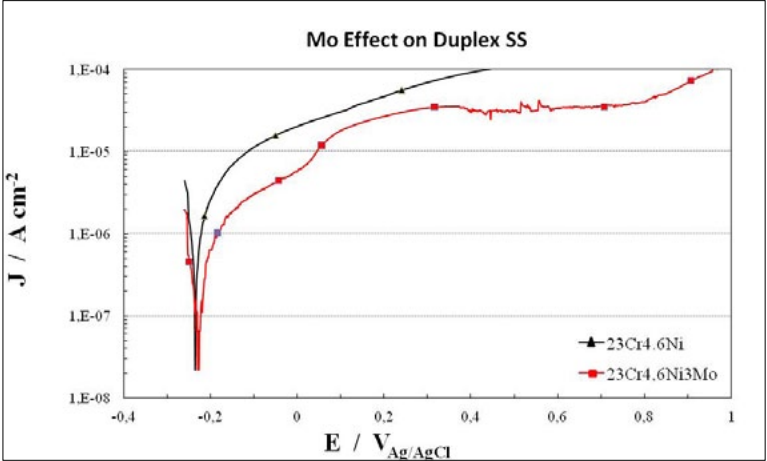






Fig. 13 - Polarization curves obtained for 23Cr4.6Ni (black) and 23Cr4.6Ni3Mo (red) SS in chloride contaminated and carbonated concrete. The Mo effect can be directly observed by comparing these curves.

3.3. Scanning Electron Microscope (SEM) study of the crevice corrosion surfaces

Some samples were examined in a scanning electron microscope (SEM) with a chemical analysis by energy dispersive spectroscopy (EDS). Fig. 14 shows the corroded surface of the austenitic SS, with and without Mo. It can be clearly seen that the crevice corrosion is located in the steel/resin interface for both steels. A chemical analysis of the corrosion products in the crevice zone of the 18Cr12Ni and 18Cr12Ni3Mo was done and the obtained results are presented in Table 6.

As expected, a high concentration of chlorides and oxygen were found in the corroded zones. The presence of these elements has an important effect on the initiation and propagation of the corrosion attack. Moreover, the oxygen content obtained in the crevice corrosion of 18Cr12Ni sample is much higher compared to the 18Cr12Ni3Mo SS, which means that the crevice zone of 18Cr12Ni SS probably presented more oxides (strong formation of corrosion products) than the same zone of the 18Cr12Ni3Mo SS. This behaviour can be explained by

Table 5 - Optical images of the duplex stainless steel surfaces before and after anodic polarization.

NONPOLARIZED DUPLEX SS		
	23Cr4.6Ni – sample 8	23Cr4.6Ni 3Mo – sample 4
E_{corr}	-124 mV _{SCE}	-144 mV _{SCE}
Images		
	Slight Crevice Corrosion	No corrosion
DUPLEX SS AFTER ANODIC POLARIZATION		
	23Cr4.6Ni – sample 7	23Cr4.6Ni 3Mo – sample 7
Images		
	High Crevice Corrosion	No corrosion

the fact that both aspects of the localized corrosion (initiation and propagation) were probably slowed down by the presence of Mo within the crevice. It is important to point out that the 18Cr12Ni3Mo austenitic SS presented a significant Mo content in the crevice as shown in Table 6.

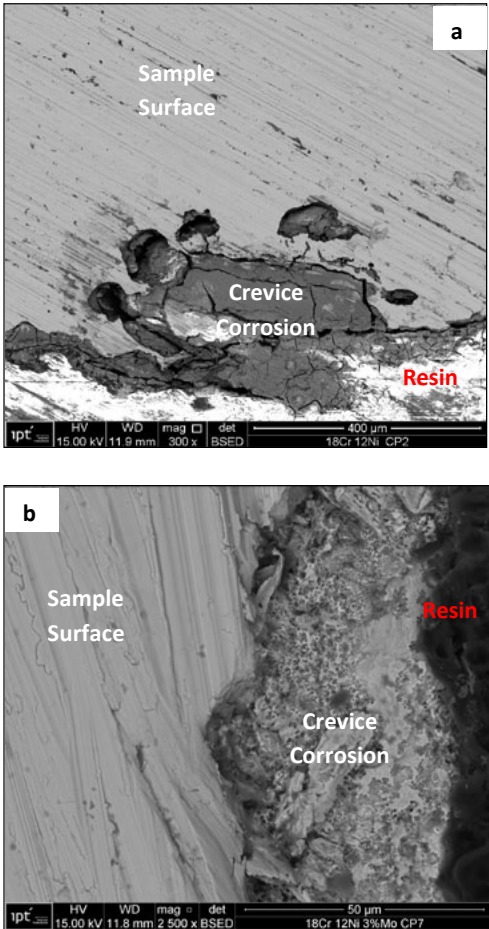


Fig. 14 - SEM of the crevice corrosion occurred in the metal/resin interface for a) 18Cr12Ni and b) 18Cr12Ni3Mo austenitic stainless steels after anodic polarization.

Table 6 - Elements detected on the crevice zone by EDS measurements.

Steel	Element (wt %)										
	C	O	Al	Si	S	Cl	Cr	Mn	Fe	Ni	Mo
18Cr12Ni	8.82	62.92	0.13	0.75	2.35	1.98	14.12	-	6.87	2.05	-
18Cr12Ni3Mo	22.94	7.51	-	0.39	-	0.38	15.54	1.76	44.22	5.53	1.73

3.4. Final comments

The first experiments developed in a carbonated and chloride-contaminated concrete help the authors to have a better understanding of the Mo behaviour on the localized corrosion for the different SS types. However, further work must be done in order to confirm the results presented above and also to establish a final protocol to evaluate the stainless steel corrosion resistance in the concrete which is a complex medium. A special attention must be given in the preparation of concrete covered metallic specimens in order to avoid crevice formation at the steel/resin interface. This will permit evaluating the pitting corrosion resistance of the studied alloys without the interference of the crevice corrosion. Further experiments should be carried out in order to promote the use of different stainless steels instead of carbon steel in concrete structures exposed to aggressive corrosion areas, such as, coastal cities and bridges.

4. CONCLUSION

As far as the experiments done in the concrete environment are concerned, the 3 % Mo addition increased the crevice corrosion resistance for all laboratory SS families even for the austenitic ones, which presented anomalous results in the synthetic carbonated pore concrete solution (pH 10) [1].

The 23Cr4.6Ni3Mo (EN 1.4462) duplex stainless steel presented the highest corrosion resistance among all studied materials under the studied aggressive concrete condition (after carbonation and immersion in the 35 g L⁻¹ of NaCl solution).

Almost all of the samples presented crevice corrosion in the metal/resin interface. Therefore, the experimental methodology should be improved in order to avoid the crevice corrosion during the electrochemical experiments.

Acknowledgments

The authors wish to thank the UGITECH Company for financial and technical support for this project.

REFERENCES

[1] T. J. Mesquita, E. Chauveau, M. Mantel, N. Kinsman and R. P. Nogueira, *Mater. Chem. Phys.*, 126, 602 (2011).
[2] D. Addari, B. Elsener and A. Rossi, *Electrochim. Acta*, 53, 8078 (2008).
[3] C. J. Abbott, *Concrete*, 31, 28 (1997).
[4] G. Blanco, A. Bautista, and H. Takenouti, *Cement Concrete Comp.*, 28, 212 (2006).
[5] A. Pardo, M. C. Merino, A. E. Coy, F. Viejo, R. Arrabal and E. Matykina, *Corros. Sci.*, 50, 780 (2008).
[6] A. Pardo, M. C. Merino, A. E. Coy, F. Viejo, R. Arrabal and E. Matykina, *Corros. Sci.*, 50, 1796 (2008).
[7] G. P. Halada, C. R. Clayton and H. Herman, *J. Electrochem. Soc.*, 142, 74 (1995).
[8] W. A. Badawy and F. M. Al-Kharafi, *Electrochim. Acta*, 44, 693 (1998).
[9] G. O. Ilevbare and G. T. Burstein, *Corros. Sci.*, 43, 485 (2001).
[10] C. Lemaitre, A. A. Moneim, R. Djoudjou, B. Baroux and G. Beranger, *Corros. Sci.*, 34, 1913 (1993).
[11] E. Chauveau, T. Sourisseau, B. Dermelin and M. Mantel (Lean Duplex Stainless Steels for Concrete Reinforcement) in *Proceedings of International Conference in Coastal and Marine Environments*, USA (2008).
[12] T. J. Mesquita, E. Chauveau, M. Mantel, N. Kinsman and R. P. Nogueira (Influence of Mo Alloying on Pitting Corrosion of Stainless Steels used as Concrete Reinforcement) in *Proceedings of European Corrosion Congress*, Stockholm, Sweden (2011).
[13] A. Araujo and Z. Panossian (Avaliação de Desempenho de Verniz Acrílico e Verniz Poliuretano Anti Antipichação como Revestimentos de Proteção às Estruturas de Concreto Aparente) in *Proceedings of Congresso Brasileiro de Corrosão*, Recife, Brazil (2008).
[14] ABNT NBR 5739:1994. (Concreto: ensaio de compressão de corpos-de-prova cilíndricos), ABNT, Rio de Janeiro, Brazil (1994).
[15] ABNT NBR NM 248:2003. (Agregados: determinação da composição granulométrica), ABNT, Rio de Janeiro, Brazil (2003).
[16] ABNT NBR 11578:1997. (Cimento Portland Composto: especificação), ABNT, Rio de Janeiro, Brazil (1997).
[17] T. J. Mesquita, A. Araujo, Z. Panossian, R. P. Nogueira, A. S. D. Junior, D. R. N. Filho e S. C. S. Dias. (Estudo da Influência do Molibdênio na Resistência à Corrosão de Aços Inoxidáveis Ferríticos, Austeníticos e Dúplex em Solução Simulada de Água de Poro e em Concreto) in *Proceedings of Congresso Internacional de Corrosão*, Salvador, Brazil (2012).